Filter-less WDM for Visible Light Communications using Coloured PAM

[1]Andrew Burton*, [2]Paul Anthony Haigh, [3]Petr Chvojka, [1]Zabih Ghassemlooy, [3]Stanislav Zvánovec

[1]*Optical Communications Research Group, Department of Electrical and electronic Engineering, Faculty of Engineering and Environment, Northumbria University, Newcastle upon Tyne, NE1 8ST, UK*
[2]*Intelligent sensing and communications group, Faculty of Science, Agriculture and Engineering, Newcastle University, Newcastle upon Tyne, NE1 7RU, UK*
[3]*Wireless and Fiber Optics group, Department of Electromagnetic Field, Faculty of Electrical Engineering, Czech Technical University in Prague, Prague 16627, Czech Republic*
**Corresponding author: andrew2.burton@northumbria.ac.uk*

Received 07 Month 2019; revised XX Month, XXXX; accepted XX Month XXXX; posted XX Month XXXX (Doc. ID XXXXX); published XX Month XXXX

This paper demonstrates, for the first time, a new wavelength-division multiplexing (WDM) scheme for visible light communications using multi-level coloured pulse amplitude modulation (*M*-CPAM). Unlike traditional WDM, no optical bandpass filters are required and only a single optical detector is used. We show that, by transmitting *n* independent sets of weighted on-off keying non-return-to-zero data on separate wavelengths over a line-of-sight transmission path, the resultant additive symbols can be successfully demodulated. Hence, the data rates can be aggregated for a single user or divided into individual colours for multiple user access schemes. The system is empirically tested for *M* = 4 and 8 using an off-the-shelf red, green and blue (RGB) chip light emitting diode (LED). We demonstrate that for *M* = 4, using the R and B chips a bit error rate (BER) of ≤10^{-6} can be achieved for each wavelength at bit rates up to 10 Mbps, limited by the LEDs under test. For *M* = 8 using R, G and B a BER of ≤10^{-6} can be achieved for each wavelength at bit rates up to 5 Mbps. The reduction in the bit rate is due to the additional signal-to-noise ratio requirement for the additional symbol levels.

http://dx.doi.org/10.1364/OL.99.099999

1. INTRODUCTION

Visible light communications (VLC) relies on using the visible spectrum for wireless data communications, to which light-emitting diodes (LEDs) are commonly used [1]. Applications include indoor communications and device-to-device communications [2]. However, LEDs with a phosphor coating to colour convert blue LEDs (WPLEDs), have a slow transient response resulting in a limited modulation bandwidth B_{mod} typically 2-3 MHz [1, 3]. Another scheme utilises red, green and blue (RGB) LEDs with significantly higher B_{mod} up to an order of magnitude higher than WPLEDs [4]. Several methods have been proposed to increase B_{mod} in both types of device including equalisations [5-7], blue filtering [8], parallel transmission (i.e., multiple-input multiple-output (MIMO)), wavelength-division multiplexing (WDM) [1, 9-11] and colour shift keying (CSK) [11] or more spectrally efficient advanced modulation formats [1, 13]. Generally, when using equalisation techniques, there is a trade-off between B_{mod}, gain and power loss in order to avoid system complexity due to the increased additional computational load [14]. Parallel transmission represents another attractive option where very high aggregated data rates of 6.36 Gb/s have been reported [8]. However, this is a hardware intensive method, which requires *n* transmitters (Txs) and *m* receivers (Rxs). RGB LEDs naturally lend themselves to parallel WDM transmission and there have been many reports on this in the literature [9, 15-18]. Likewise, CSK systems have been reported where different combinations of the Tx wavelengths represent individual points of a constellation [11] based on a two-dimensional chromatic space. However, in these works (WDM and CSK), an individual Rx and optical bandpass filter (OBF) have been utilised for each wavelength multiplexed, as well as lenses, which make the systems costly and bulky. Nonetheless, WDM systems have been reported with higher data rates (>16 Gb/s) [18].

The problem with OBFs is that, they are expensive and must be matched to the individual wavelengths used. Employing multiple photodetectors (PDs) is also undesirable due to the increased hardware complexity. Therefore, in this paper, we propose a new approach for implementation of WDM-based

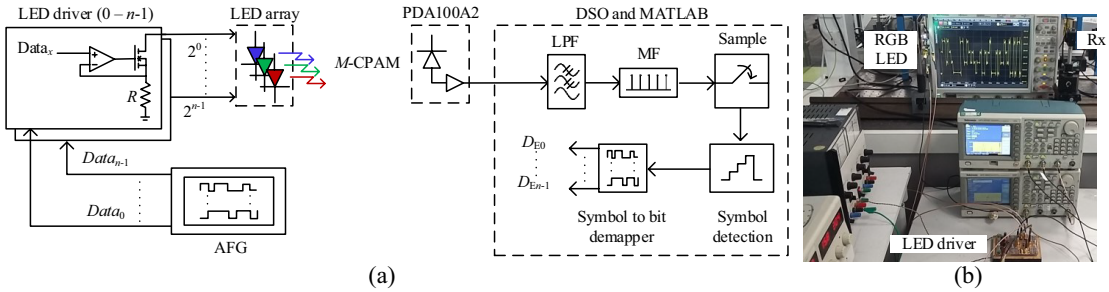

Fig. 1 (a) Experimental *M*-CPAM system block diagram, AFG: arbitrary function generator, MF: matched filter, DSO: digital storage oscilloscope; and (b) photograph of experimental setup.

VLC, which requires no OBF and uses only a single optical Rx independent of the number of transmitting LEDs (i.e., wavelengths). Hence, the hardware requirement is reduced by a factor of *m*. The received WDM signal consists of superposed symbols, comprising of the sum of *n* pseudorandom binary sequences (PRBS) on-off keying non-return to zero (OOK-NRZ) signals, which occupy the same frequency space. We call the resultant format multi-level colour pulse amplitude modulation (*M*-CPAM). In *M*-CPAM symbols are demodulated using a hard thresholding technique adopted from the conventional PAM scheme prior to being demultiplexed into original data streams, depending upon the weighting of the symbol-to-bit de-mapping. This technique can be used to either aggregate the data streams and increase the bit rate R_B for a single user or to assign different wavelengths to different users.

The rest of the paper is organised as follows. Section 2 outlines the proposed *M*-CPAM, Section 3 describes the experimental test-bed, results and discussion are given in Section 4, and finally, the conclusion is outlined in Section 5.

2. COLOURED PULSE AMPLITUDE MODULATION

The schematic block diagram for the proposed line of sight (LoS) CPAM VLC link is shown in Fig. 1(a). For intensity modulation of *n* LEDs (i.e., RGB with different defined wavelengths), *n* independent OOK-NRZ data streams are used. Note, LEDs are intentionally weighted with respect to each other. This is to ensure that, at the output of the Rx (i.e., transimpedance amplifier (TIA)) the regenerated electrical signals from LED_0 to LED_{n-1} have relative amplitude weights of 2^0 to 2^{n-1}, respectively. Hence, the relative signal amplitudes are doubled with every additional LED to maintain the appropriate Euclidean distance. The overall CPAM order is given by $M = 2^n$.

The weighting of each LED at the peak wavelength is set by the modulation depth (MD) and the biasing current I_{bias}. The order of weighting of LEDs is determined using (*i*) the responsivity $\mathcal{R}(\lambda)$ of the silicon PD, see Fig. 2(a), for B (469 nm), G (529 nm) and R (645 nm) peak wavelengths, and (*ii*) the normalised optical power-current (*P-I*) characteristics (i.e., electro-optic (E/O) conversion) of the RGB LEDs as depicted in Fig. 2(b). For the experiment using the B and R LEDs, which have similar *P-I* profiles and $\mathcal{R}$ of ~0.24 and ~0.46 A/W, respectively are therefore assigned with the relative weighting orders of 2^0 and 2^1, respectively. On the other hand, when using BRG LEDS with the G LED having the lowest *P-I* profile and $\mathcal{R}$ of ~0.32 A/W, the assigned weighting order are 2^1, 2^2 and 2^0, respectively. Note, for different LEDs the relative weights order assignment should be based on the *P-I* characteristics and $\mathcal{R}$.

For 4-CPAM, the recovered electrical signals ($y_B(t)$ and $y_R(t)$) at the output of the TIA for the B and R LED Txs, respectively are given by:

$$y_B(t) = \left(x_B(t)w_b \otimes h_c(t)\right)\mathcal{R}(469) + n(t), \quad \textbf{(1)}$$

$$y_R(t) = \left(x_R(t)w_r \otimes h_c(t)\right)\mathcal{R}(645) + n(t), \quad \textbf{(2)}$$

where $x_B(t)$ and $x_R(t)$ are the IM optical signal for B and R LEDs with respective weights of w_b and w_r. The symbol $\otimes$ is the time domain convolution, and $h_c(t)$ is the channel impulse response (considered to be fixed based on the experimental setup and the LEDs used). $n(t)$ is the additive white Gaussian noise, where the background induced shot noise is the dominant source in VLC, whose variance is defined by [1]:

$$\sigma_{bg}^2 = 2qB_{ef}\mathcal{R}I_{bg}, \quad \textbf{(3)}$$

where q is the electron charge, B_{ef} is the bandwidth of the electrical filter following the optical Rx and I_{bg} is the background induced photocurrent.

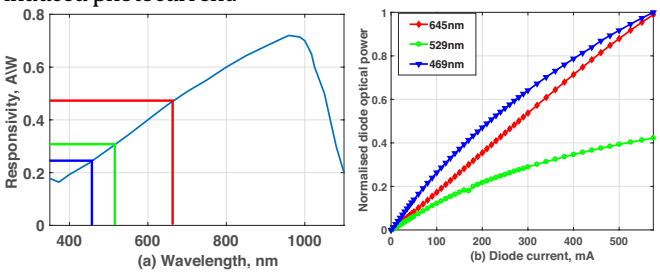

Fig. 2 (a) $\mathcal{R}(\lambda)$ curve of PDA100A2 Si PD and (b) normalised power-current (E/O conversion) response of the RGB LEDs.

At the PD both received optical signals are linearly summed and the resultant electrical CPAM signal is given by:

$$y_{CPAM}(t) = y_B(t) + y_R(t). \quad \textbf{(4)}$$

Alternatively, in a more general form, for *n* wavelengths:

$$y_{CPAM}(t) = \sum_{i=0}^{n-1} y_i(t), \quad \textbf{(5)}$$

where *i* is the colour index.

Demodulation of CPAM is simple and takes place in two stages of (*i*) detection and mapping of the received superposed

CPAM signal into M possible symbol levels based on the conventional PAM decoding scheme, i.e., hard threshold detection (see Fig. 3); and (*ii*) converting the received symbols into their weighted colour-specific binary sequences using the look-up table (Table I), which demonstrates the conversion of symbols to the estimated data for $M = 4$, using the R and B LEDs.

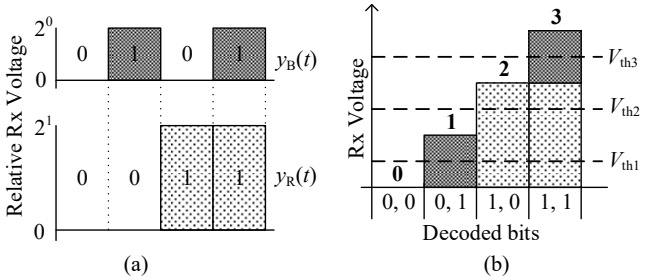

Fig. 3 (a) the individual Rx OOK NRZ for the $y_R(t)$ and $y_B(t)$ and (b) the Rx additive $y_{CPAM}(t)$ symbols for $M = 4$ where V_{thx} are the hard threshold levels (symbols are shown in bold).

Table I CPAM symbol to data bit conversion for $M = 4$

Symbol	R	B
0	0	0
1	0	1
2	1	0
3	1	1

Following the binary demapping of the symbols, the data on the weighted signals on channels 0 and (n-1) carry the least significant bit (LSB) and the most significant bit (MSB), respectively. Furthermore, there are three constraints to ensure successful transmission of the M-CPAM signals that must be satisfied: (*i*) they have the same bit rate; (*ii*) are fully synchronised at the Tx; and (*iii*) have accurate relative electrical amplitudes at the Rx (i.e., 2^0, 2^1, … 2^{n-1}).

3. EXPERIMENTAL SETUP

The experimental test-bed for evaluation of the proposed LoS CPAM VLC system for $M = 4$ and 8 is shown in Fig. 1(a). Each of the n PRBS of length 2^{10}-1 is generated in MATLAB and uploaded onto two synchronised AFG's (Tektronix AFG3252). The electrical signals are used for IM of off the shelf RGB LED via a DC coupled MOSFET output driver, see Fig. 1. Both the DC offset current I_{DC} and MD are controlled at the AFG. Following free-space transmission (with the channel impulse response $h_c(t)$), the signal is detected using an optical Rx (i.e., Thorlabs - PDA100A2). The regenerated electrical signal $y_{ele}(t)$ is captured and recorded using a DSO (Agilent Technologies Infiniium DSO9254A) for off-line processing in MATLAB. The signal processing includes symbol timing and frame synchronisation, low-pass filtering (LPF) at the cut-off frequency $f_{c\text{-}LPF}$ equal to the Baud rate R_{Bd}, MF and down-sampling prior to symbol detection and bit mapping to estimate the transmitted data streams. Experimental parameters are given in Table II.

In the experiment for $M = 4$, the R LED is IM with a maximum drive current of the driver circuit given in Table II. In order to maintain the received relative weight, the output of the B LED is adjusted such that the regenerated electrical OOK NRZ signal has precisely half the amplitude of the regenerated electrical signal from the R LED. For $M = 8$, the same conditions have been kept for the IM R and B LEDs with the amplitude of the regenerated electrical OOK NRZ signal from the G LED being set at half of the signal from the B LED.

Table II Critical experimental parameters

Parameter	Value
Experiment 1, $M = 4$ (Experiment 2, M=8)	
LED type	R, B (and G)
LED bias current, I_{bias}	R = 330 mA B = 230 mA (G = 170 mA)
Modulation depth	All = 100%
Channel length (LoS)	50 cm
Rx BW	11 MHz
PD's responsivity, $\mathcal{R}(\lambda)$	@ 645 nm 0.46 A/W @ 469 nm 0.24 A/W (@ 529 nm 0.32 A/W)
Rx noise equivalent power @ 960 nm	7.17×10^{-11} WHz^{-2}

4. EXPERIMENTAL RESULTS

4.1 LED characterisation

The LEDs used in this work were characterised as illustrated in Fig. 4(a)-(b) for the frequency response and optical spectrum, and in Fig. 2(b) for E/O conversion. The measured frequency response at the output of the optical Rx (Agilent Technologies MXA Signal analyser (N9020A)) is shown in Fig. 4(a). The traces are normalised to 0 dB at the minimum test frequency of 300 kHz. The measured 3 dB bandwidths are 11.4, 10.1 and 10.7 MHz for the R, B and G LED chips, respectively. Fig. 4(b) was measured using a ThorLabs CCS200/M spectrometer with each LED chip DC biased as stated in Table II. The traces are normalised using the maximum measured level of the B LEDs response. It can be seen from Fig. 4(b) that, each colour is almost completely isolated from the others, with only the G and B LEDs showing partial overlap and therefore with possible inter-colour crosstalk (as in WDM).

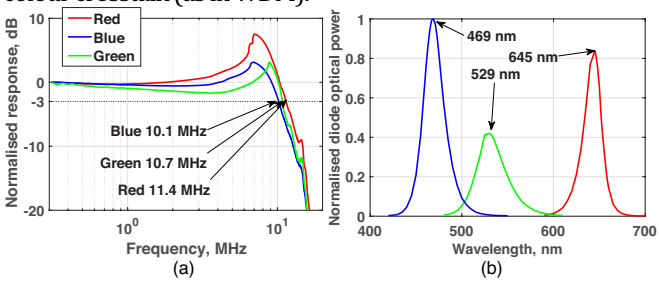

Fig. 4 The RGB LED: (a) frequency response and (b) optical spectrum.

4.2 M-CPAM VLC

The BER plots for the proposed M-CPAM system are shown in Figs. 4(a) and (d) following symbol detection and bit-mapping process outlined in Table I. A BER error floor of 10^{-6} is set, and a

minimum of 2×10^6 symbols have been tested for each R_{Bd}. Fig. 5(a) illustrates that for the R and B wavelengths the data is successfully demultiplexed and demodulated from the composite signal up to the R_{Bd} of 10 MBd at a BER ≤ 10^{-6}. The R_{Bd} increases to ~12 MBd at the 7% forward error correction (FEC) BER limit of 3.8×10^{-3}. Fig. 5(a) also depicts that, both colours exhibit an almost identical BER performance, regardless of the fact that the B has been regenerated with half the amplitude of the R. Hence, when used as a multiple access scheme the available resources are fairly distributed between both users while experiencing the same BER. Alternatively, for a single user, R_B has been effectively doubled. Figs. 5(b) and (c) display the eye diagrams at 1 sample/bit for the received symbols at 5 and 15 MBd (BERs of ≤10^{-6} and ~10^{-2}), respectively (eye diagrams were captured following down-sampling, see Fig. 1). Note, in Fig. 5(c) the eye diagram is almost closed hence the increased BER.

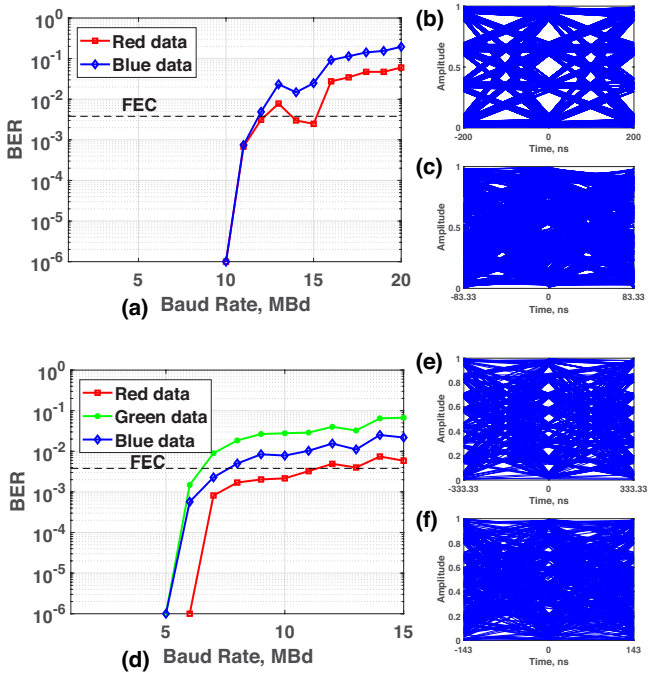

Fig. 5 BER vs. R_{Bd} with the eye diagrams for (a) 4-CPAM with (b) 5 MBd and (c) 15 MBd; and (d) 8-CPAM with (e) 3 MBd and (f) 7 MBd.

The results for $M = 8$ are shown in Fig. 5(d)-(f) using the RGB LED chips. Clearly for a BER ≤ 10^{-6} the demultiplexed and demodulated signals are up to 5 MBd below the level set for $M = 4$. This can be explained by the fact that, the power levels of the R and B signals are identical to $M = 4$, however, with the addition of the received G signal at half the amplitude of the B signal, the Euclidian distance between the signal levels has effectively been halved. Hence, there are additional levels in the same signalling space. Thus, the signal to noise ratio (SNR) has been radically reduced. This can be seen in the eye diagrams displayed in Figs. 5(e) and (f) with R_{Bd} of 3 and 7 MBd, respectively. The reasoning behind the signal levels is that, the R signal was set to the maximum output power (i.e., highest driver current), which sets the constraints on the B and G signal levels. Nevertheless, we postulate that, a Tx with the capability to drive the R signal at higher drive current (i.e., higher power levels), the same Euclidian distance between the signal levels could be obtained (as in $M = 4$), thus leading to vastly improved SNR and BER performance. Additionally, for $M = 8$, the aggregate bit rate for the case of a single user has been increased by a factor of 3 (i.e. $\log_2 M$), and for the multiuser scenario once again the separate data streams show an almost identical BER performance regardless of the transmit power.

It must also be noted here that, the aim of this paper has not been to show transmission of higher data rate than reported in the literature, but to demonstrate that WDM-based VLC can be implemented without the need for OBF's and multiple receivers. Thus, leading to increased system throughput per single user or adding additional users relative to the number of wavelengths.

5. CONCLUSIONS

This paper demonstrated the implementation of a new technique for WDM-based VLC using M-CPAM without the requirement for multiple receivers each equipped with costly specially tuned OBF's. The theoretical concept for M-CPAM was described and experimentally demonstrated. For 4-CPAM, two colours of red and blue were used; likewise, for 8-CPAM, we used three colours of red, blue and green. We demonstrated a BER of ≤ 10^{-6} for the symbol rates of 10 MBd and 5 MBd for M = 4 and 8, respectively. The results also demonstrated a similar BER performance between each of the data streams associated with a particular order of M, thus showing each colour utilising both the bandwidth and amplitude resources fairly.

ACKNOWLEDGEMENT

This project is supported by UK EPSRC grant EP/P006280/1: MARVEL, the Czech Science Foundation GACR 17-17538S and the H2020 MSC ITN 764461 (VISION).

REFERENCES

1. Z. Ghassemlooy, W. Popoola, and S. Rajbhandari, Optical wireless communications: system and channel modelling with Matlab, (CRC Press, 2019.), 2nd ed.
2. G. Corbellini, K. Aksit, S. Schmid, et al., IEEE Commun. Mag. 52, 72 (2015).
3. D. Karunatilaka, F. Zafar, V. Kalavally, and R. Parthiban, IEEE Commun. Surveys Tuts. 17, 1649 (2015).
4. Z. Ghassemlooy, L. N. Alves, S. Zvanovec, and M.-A. Khalighi, Visible Light Communications: Theory and Applications (CRC Press, 2017), 1st ed.
5. C. Han, X. Sun, and S. Cui, in IEEE ICSAI, (IEEE, 2017), 1035.
6. X. Li, N. Bamiedakis, X. Guo, et al., J. Lightw. Technol. 34, 2049 (2016).
7. Z. Yingjun, L. Shangyu, C. Siyuan, X. Huang, and N. Chi, in IEEE WOCC, (IEEE, 2016) 1.
8. S. Wang, F. Chen, L. Liang, et al., IEEE Wireless Commun. 22, 61 (2015).
9. I. Lu, C. Lai, C. Yeh, and J. Chen, in OFC, (IEEE, 2017) 1.
10. N.Omura, A. Higashi, J. Yabuuchi, T. Iwamatsu, and S. Oshiba, APMC, (IEEE, 2018) 872.
11. K. Werfli, P. Chvojka, Z. Ghassemlooy, et al, J. Lightw. Technol. 36, 1944 (2018).
12. R. Singh, T. O'Farrell, J.P.R David, J. Lightw. Technol. 32, 2582 (2014)
13. P. Haigh, P. Chvojka, Z. Ghassemlooy, et al., Opt. Expr. 27, 8912 (2019).
14. P. A. Haigh, Z. Ghassemlooy, H. L. Minh, et al., J. Lightw. Technol. 30, 3081 (2012).
15. V. S. R. Krishna and R. Singhal, in IEEE WOCN, (IEEE, 2016) 1.
16. Z. Li, D. Sun, H. Yang, and J. Song, in 2017 IEEE BMSB, (IEEE, 2017) 1.
17. C. Tang, M. Jiang, H. Shen, and C. Zhao, IEEE Photon. J. 7, 1 (2015).
18. R. Bian, I. Tavakkolnia, and H. Haas, J. Lightw. Technol. 37, 2418 (2019).

FULL REFERENCES

1. Z. Ghassemlooy, W. Popoola, and S. Rajbhandari, *Optical wireless communications: system and channel modelling with Matlab®,* 2nd ed. (CRC Press, USA, 2019).
2. G. Corbellini, Kaan Aksit, S. Schmid, S. Mangold, T.R. Gross, “Connecting networks of toys and smartphones with visible light communication,” IEEE Communications Magazine **52**, 72-78 (2014).
3. D. Karunatilaka, F. Zafar, V. Kalavally, and R. Parthiban, "LED Based Indoor Visible Light Communications: State of the Art," IEEE Communications Surveys & Tutorials **17**, 1649-1678 (2015).
4. Z. Ghassemlooy, L. N. Alves, S. Zvanovec, and M.-A. Khalighi, *Visible Light Communications: Theory and Applications* (CRC Press, 2017).
5. C. Han, X. Sun, and S. Cui, "Design of 100Mbps white light LED based visible light communication system," in *2017 4th International Conference on Systems and Informatics (ICSAI)*, 2017), 1035-1039.
6. X. Li, N. Bamiedakis, X. Guo, J. J. D. McKendry, E. Xie, R. Ferreira, E. Gu, M. D. Dawson, R. V. Penty, and I. H. White, "Wireless Visible Light Communications Employing Feed-Forward Pre-Equalization and PAM-4 Modulation," Journal of Lightwave Technology **34**, 2049-2055 (2016).
7. Z. Yingjun, L. Shangyu, C. Siyuan, X. Huang, and N. Chi, "2.08Gbit/s visible light communication utilizing power exponential pre-equalization," in *2016 25th Wireless and Optical Communication Conference (WOCC)*, 2016), 1-3.
8. S. Wang, F. Chen, L. Liang, S. He, Y. Wang, X. Chen, Wei Lu, “A high-performance blue filter for a white-led-based visible light communication system,” IEEE Wireless Communications **22**, 61-67 (2015).
9. I. Lu, C. Lai, C. Yeh, and J. Chen, "6.36 Gbit/s RGB LED-based WDM MIMO visible light communication system employing OFDM modulation," in *2017 Optical Fiber Communications Conference and Exhibition (OFC)*, 2017), 1-3.
10. N. Omura, A. Higashi, J. Yabuuchi, T. Iwamatsu, and S. Oshiba, "Experimental Demonstration of OFDM Based WDM-MIMO Visible Light Communication System," in *2018 Asia-Pacific Microwave Conference (APMC)*, 2018), 872-874.
11. K. Werfli, P. Chvojka, Z. Ghassemlooy, N. B. Hassan, S. Zvanovec, A. Burton, P. A. Haigh, and M. R. Bhatnagar, "Experimental Demonstration of High-Speed 4 × 4 Imaging Multi-CAP MIMO Visible Light Communications," Journal of Lightwave Technology **36**, 1944-1951 (2018).
12. R. Singh, T. O’Farrell, J.P.R David, “An Enhanced Color Shift Keying Modulation Scheme for High-Speed Wireless Visible Light Communications,” Journal of Lightwave Technology **32**, 2582 - 2592 (2014).
13. P. Haigh, P. Chvojka, Z. Ghassemlooy*, et al.*, "Visible light communications: multi-band super-Nyquist CAP modulation," Optics Express **27**, 8912-8919 (2019).
14. P. A. Haigh, Z. Ghassemlooy, H. L. Minh, S. Rajbhandari, F. Arca, S. F. Tedde, O. Hayden, and I. Papakonstantinou, "Exploiting Equalization Techniques for Improving Data Rates in Organic Optoelectronic Devices for Visible Light Communications," Journal of Lightwave Technology **30**, 3081-3088 (2012).
15. V. S. R. Krishna and R. Singhal, "720-Mbps 64-QAM-OFDM SCM transmission over RGB-LED-based FSO communication system," in *2016 Thirteenth International Conference on Wireless and Optical Communications Networks (WOCN)*, 2016), 1-5.
16. Z. Li, C. Zhang, D. Sun, H. Yang, and J. Song, "A real-time high-speed visible light communication system based on RGB-LEDs," in *2017 IEEE International Symposium on Broadband Multimedia Systems and Broadcasting (BMSB)*, 2017), 1-4.
17. C. Tang, M. Jiang, H. Shen, and C. Zhao, "Analysis and Optimization of P-LDPC Coded RGB-LED-Based VLC Systems," IEEE Photonics Journal **7**, 1-13 (2015).
18. R. Bian, I. Tavakkolnia, and H. Haas, "15.73 Gb/s Visible Light Communication With Off-the-Shelf LEDs," Journal of Lightwave Technology **37**, 2418-2424 (2019).